



Reprint 542

The effect of ENSO and East Asian Monsoon  
on the Annual Rainfall in Hong Kong, China

Y.K. Leung & M.C. Wu

Sixth Joint Meeting of Seasonal Prediction on  
East Asian Summer Monsoon, Guilin, China, 11-13 May 2004

# **The effect of ENSO and East Asian Monsoon on the Annual Rainfall in Hong Kong, China**

Leung Yin Kong<sup>1</sup>, Wu Man Chi

*Hong Kong Observatory*

*134A Nathan Road, Tsimshatsui, Hong Kong, China*

## **1. Introduction**

1997 was the wettest year in Hong Kong since records began in 1884. The rainfall at the Hong Kong Observatory amounted to 3343 mm, 51 per cent above the 30-year (1961-1990) mean of 2214 mm. That this exceptional heavy rain in Hong Kong coincided with the onset of one of the strongest El Nino events in the 20<sup>th</sup> century has aroused interest in the possible link between El Nino-Southern Oscillation (ENSO) phenomenon and the annual rainfall in Hong Kong.

Previous study by Chang and Yeung (2003) demonstrated the effects of ENSO and the strength of winter monsoon in the preceding winter on the annual rainfall in Hong Kong. Building on their work, this study updates and elaborates on their findings. The associated physical basis linked to the variation of monthly rainfall is also explored.

## **2. Data and definitions**

In this study, 54 years (1950-2003) of Hong Kong's rainfall data from the Hong Kong Observatory are used. The rainfall data in Mainland China are sourced from the National Climate Centre (NCC) of China Meteorological Administration (CMA).

The monthly Nino-3.4 sea surface temperature anomaly (SSTA) data are available from the United States Climate Prediction Center's web site at <http://ftp.ncep.noaa.gov/pub/cpc/wd52dg/data/indices/sstoi.indices>. The United States National Centers for Environment Prediction-National Center for Atmospheric Research (NCEP-NCAR) re-analysis data are used in the

---

<sup>1</sup> Leung Yin Kong, tel.: (852) 2926 3112, fax: (852) 2311 9448, email: jykleung@hko.gov.hk

analysis of large-scale surface as well as upper-air conditions. These re-analysis data are gridded data with a horizontal resolution of  $2.5^\circ \times 2.5^\circ$ . A detailed description of the data can be found in Kalnay et al. (1996). As pointed out by Trenberth and Caron (2000), the NCEP-NCAR re-analysis data prior to 1958 are not of good quality and hence they are not used in the present study. The data from 1958 to 1996 are extracted from the CD-ROM containing 40 years (1957-1996) of the re-analysis data which was included in Vol. 77(3) of the Bulletin of American Meteorological Society. The data from 1997 onwards are downloaded from the NCEP web site (<http://www.cdc.noaa.gov/cdc/data.ncep.reanalysis.html>).

Following Chang and Yeung (2003), the annual rainfall in Hong Kong in the present study is classified into three categories: below normal, near normal and above normal. Near normal is defined as the long-term (1961-1990) mean plus/minus half a standard deviation, i.e. 1958 mm to 2470 mm. Annual rainfall less than 1958 mm is classified as below normal, and over 2470 mm as above normal.

ENSO episodes and their strength are classified similarly as in Li and Zhai (2000). The classification of ENSO years since 1950 can be found in Table 1.

For the purpose of studying inter-annual variability in monsoon activity, the unified monsoon index (UMI) defined by Lu and Chan (1999) are used to represent the strength of winter monsoon over south China. UMI is defined as the meridional wind at 1000 hPa averaged over the northern part of the South China Sea ( $7.5^\circ - 20^\circ$  N,  $107.5^\circ - 120^\circ$  E). In this study, the computation of UMI is based on the NCEP re-analysis data and the strength of winter monsoon (UMI averaged over the winter months December-January-February) is classified into three categories: weak, neutral or strong according to the value of UMI. Neutral UMI is defined as the long-term (1961-1990) mean plus/minus half a standard deviation, i.e. -5.79 to -4.95. Weak and strong winter monsoon refers to UMI greater than -4.95 or below -5.79 respectively.

In this paper, spring refers to the months from March to May, summer from June to August, autumn from September to November and winter from December to February.

### **3. Periodic characteristics of annual rainfall**

Figure 1 shows the time series of annual rainfall in Hong Kong between 1950 and 2003. The annual rainfall ranges from the lowest 901 mm recorded in 1963 to the highest 3343 mm in 1997. The long-term (1961-1990) mean and standard deviation are 2214 mm and 512 mm respectively.

In this study, both wavelet and spectral analyses are conducted to investigate the periodic variations of annual rainfall in Hong Kong. The details of the method of wavelet analysis can be found in Leung and Wu (2000), and Torrence and Compo (1998). The Mexican Hat Function is used as the mother wavelet in this paper.

The results of wavelet and spectral analyses are shown in Figure 2 and 3 respectively. It can be seen from Figure 2 that for low frequency oscillation with period of about 50 years, the rainfall is in the wet phase since the early 1990s. At the periodicity of about 15-40 year, dry phases appear in the mid-1960s and late 1980s. Stronger signals are found for the periods 10-15 year and 2-7 year. Spectral analysis also reveals peaks in spectral density of periods 2.3, 3.6, 4.5 and 13.5 year (Figure 3). The peaks at around 4 and 2 years suggest possible relationship of the annual rainfall with El Nino-Southern Oscillation (ENSO) and Tropospheric Biennial Oscillation (TBO) which are closely related to monsoon activities (e.g. Chang and Li, 2000; Meehl and Arblaster, 2002). The result of this spectral analysis is in line with Shen and Lau's (1995) finding of a prominent biennial signal in the East Asian summer monsoon rainfall in southeast China. Liang and Liang (1995) also pointed out that the rainfall in Guangzhou is closely related to ENSO activity.

### **4. Effect of ENSO and East Asian monsoon**

#### *4.1 ENSO*

In examining the ENSO influence, it is useful to analyse the relationship between the annual rainfall in Hong Kong and the sea surface temperature anomaly (SSTA) in the equatorial central-eastern Pacific.

Figure 4 is a scatter diagram showing the relationship between the annual rainfall and Nino-3.4 SSTA in the preceding winter. Although the rainfall-SSTA association is low (correlation coefficient  $r = 0.15$ ), a statistically significant linear relationship at 0.01 level ( $r = 0.61$ ) is noted for cases with  $SSTA > 0.6^{\circ}\text{C}$ . This shows that a linear relationship between the annual rainfall and the SSTA exists following the maturity of an El Nino episode which normally occurred in winter.

The ENSO linkage between the annual rainfall in Hong Kong and large-scale atmospheric circulation can also be recognized from Figure 5 which depicts the correlation map of the annual rainfall with the 850 hPa wind field in the preceding winter. The cyclonic dipole in the equatorial central Pacific represents the weakening of trade wind in the Walker circulation and is one of the characterizing signatures of ENSO warm phase. The anticyclonic circulation in the vicinity of Japan is related to the coupling between the East Asian winter monsoon and ENSO such that the former is likely to be weaker (stronger) during ENSO warm (cold) condition (e.g., Ding, 1994; Li et al., 2001). More detailed discussion of the relationship between rainfall and winter monsoon will be given in Section 4.2.

Table 2 tabulates the category of annual rainfall amount in relation to ENSO activity. It suggests that the annual rainfall in Hong Kong tends to be above normal in strong El Nino onset years (E0), near normal or above normal in the years immediately following El Nino onset year (E1) irrespective of strength of the El Nino event, and near normal in the years immediately following La Nina onset year (L1) irrespective of strength of the La Nina event.

Figure 6 shows the composite distribution of the rainfall in Hong Kong for different months in strong E0 years. The tendency to see above normal rainfall in strong E0 year is apparent when large positive rainfall anomalies are observed for the months May to August. The corresponding rainfall conditions for different stations in China during the same period for strong E0 years are also presented to highlight the situation at larger scale (Figure 7). Consistent with the situation in Hong Kong, the rainfall over the south China coast tends to be higher than the long-term (1961-1990) mean (i.e. positive anomaly). The composite 850 hPa wind anomaly for these months is shown in Figure 8. A cyclonic anomaly is found over the

south China coast which contributes to the above normal rainfall in Hong Kong and its vicinity.

Similar composite analyses are carried out for E1 and L1 years respectively. Unlike the case of strong E0, both episodes of positive and negative rainfall anomaly are noted for E1 years and it portrays a “first-wet and later-dry” scenario (Figure 9). This is consistent with the finding that the spring in Hong Kong is likely to be wetter than usual following the maturity of El Nino year (Lam, 1993). Figures 10a and b shows respectively the situation in China for February-July and August-October. The tendency in South China is consistent with that of Hong Kong which portrays a change from a wetter first half to drier conditions afterwards.

To explore the synoptic situation of the wetter tendency in the rainfall in the months from February to July in E1 years, the 850 hPa circulation anomaly pattern for this period is plotted (Figure 11). There is an enhanced southwesterly flow along the south China coast. These southwesterlies are due to an anomalous anticyclone over the Pacific to the east of the Philippines. This anomalous anticyclone is a typical ENSO feature which develops in the fall of E0 and persists till spring or early summer in E1 (Wang et al., 2000).

The monthly mean rainfall anomalies are comparatively smaller for L1 years than in the cases of strong E0 and E1 (Figure 12). During June-July, the rainfall condition in the vicinity of Hong Kong is less coherent spatially (Figure 13). While most stations in the eastern part of south China see a negative anomaly, positive anomaly is noted in the region northwest of Hong Kong. The drier tendency in the eastern part of South China may be attributed to the weaker than normal southwesterly flow over the region (Figure 14).

#### *4.2 East Asian winter monsoon*

While Bell (1976) was the first to relate the strength of the East Asian monsoon in the preceding winter to the summer rainfall in Hong Kong, an extension of the relationship to the annual rainfall is suggested as inferred from Figure 15. Weakening of the East Asian trough at the 500 hPa level in the vicinity of Japan is observed in the preceding winter for years with

more rainfall.

In order to eliminate the possible influence from the coupling between the winter monsoon and ENSO, only the rainfall data of the years other than strong E0, E1 and L1 mentioned in Section 4.1 are used for analysing the effect of winter monsoon on the annual rainfall in Hong Kong.

Regression analysis shows that the correlation between annual rainfall in Hong Kong and the winter UMI is 0.70, statistically significant at 0.01 level (Figure 16). From the figure, it can be seen that weaker winter monsoon in the preceding winter is associated with higher annual rainfall in Hong Kong while a stronger winter monsoon with lower annual rainfall.

For preceding weak winter monsoon years, Figure 17 shows that positive rainfall anomalies are mainly found in the summer months of June to August. During June-August, the rainfall condition in China resembles the typical type I pattern (National Climate Centre, 1999) for which southern and northern China have higher rainfall and are separated by a relatively drier belt in central China (Figure 18). This rainfall configuration is in general associated with a stronger East Asian summer monsoon (e.g., National Climate Centre, 1999). Composite analysis shows that a trough feature lies along the south China coast (Figure 19) which contributes to the positive anomaly rainfall in Hong Kong and its vicinity.

For years immediately following a strong winter monsoon, negative rainfall anomalies are observed for April to May, and July to September (Figure 20). Similarly, negative rainfall anomalies are also observed in most parts of South China during these two periods (Figure 21). For both periods, an anomalous ridge dominates along the south China coast (Figure 22) resulting in less rainfall in Hong Kong and its vicinity.

## **5. Conclusion**

The annual rainfall in Hong Kong has been found to be related to ENSO activity and the strength of winter monsoon in the preceding winter.

Statistically, the annual rainfall in Hong Kong tends to be above

normal in strong E0, near normal or above normal in E1, and near normal in L1. For the years other than strong E0, E1 and L1, the annual rainfall is statistically correlated at 0.01 significant level to the strength of the winter monsoon in the preceding winter. Weaker winter monsoon in the preceding winter is likely to be associated with higher annual rainfall in Hong Kong and stronger winter monsoon with lower annual rainfall.

An examination of the rainfall in China and the 850 hPa wind anomaly patterns reveals that the effects of ENSO and the preceding winter monsoon on the annual rainfall in Hong Kong found by Chang and Yeung (2003) also apply to the rainfall along the south China coast.

For strong E0 years, positive rainfall anomalies are observed over the south China coast for May-August which are related to the cyclonic anomaly found over the region. For E1 years, the rainfall in South China portrays a change from a wetter February-July to a drier August-October. The wetter tendency in February-July is related to the enhanced southwesterly flow along the south China coast as a result of an anomalous anticyclone over the Pacific to the east of the Philippines. This anomalous anticyclone is an ENSO-related feature which develops in the fall of E0 and persists till spring or early summer in E1.

For weak winter monsoon in the preceding winter of the years other than strong E0, E1 and L1, both southern and northern China have higher summer rainfall and are separated by a relatively drier belt in central China. A trough feature is found along the south China coast in the 850 hPa wind anomaly pattern in summer which contributes to the positive rainfall anomaly in Hong Kong and its vicinity. For years immediately following a strong winter monsoon, an anomalous ridge dominates over the south China coast in the periods April-May and July-September, resulting in less rainfall to the region.

## Acknowledgement

The authors would like to thank Mr. C.Y. Lam, Mr. K.H. Yeung and Mr. E.W.L. Ginn of the Hong Kong Observatory for their valuable comments.

## References

- Bell, G.J., 1976: Seasonal forecasts of Hong Kong summer rainfall. *Weather*, **31**, 208-212.
- Chang, C.P., and Tim Li, 2000: A theory for the tropical tropospheric biennial oscillation. *J. Atmos. Sci.*, **57**, 2209-2224.
- Chang, W.L., and K.H. Yeung, 2003: Seasonal Forecasting for Hong Kong - A Pilot Study. *Technical Note No. 104*, Hong Kong Observatory.
- Ding, Yihui, 1994: *Monsoons over China*. Kluwer Academic Publishers. 419 pp.
- Kalnay, E., and Coauthors, 1996: The NCEP/NCAR 40-year reanalysis project. *Bull. Amer. Meteor. Soc.*, **77**, 437-471.
- Lam, C.Y., 1993: El Nino/Southern Oscillation and spring weather in Hong Kong. *HKMetSoc Bulletin*, **3**, 3-13.
- Leung, Y.K., and M.C. Wu, 2000: Low-Frequency Oscillation of the Winter Monsoon in Hong Kong, China. Joint Meeting on Seasonal Prediction of the East Asian Monsoon, 21-22 November 2000, Beijing, China. *Reprint No. 367*, Hong Kong Observatory.
- Li, C.Y., S. Sun, and M.Q. Mu, 2001: Origin of the TBO-interaction between anomalous East Asian winter monsoon and ENSO cycle. *Adv. Atmos. Sci.*, **18**, 554-566 (in Chinese).

- Li, X., and P. Zhai, 2000: On indices and indicators of ENSO episodes. *ACTA Meteor. Sinica*, **58**, 102-109 (in Chinese).
- Liang, Nuanpei, and Biqi Liang, 1995: The El Nino event and rainfall variation in Guangzhou. *J. Tropical Oceanography*, **14**, 18-23 (in Chinese).
- Lu, E., and C.L. Chan, 1999: A Unified Monsoon Index for South China. *J. Climate*, **12**, 2375-2385.
- Meehl, Gerald A., and Julie M. Arblaster, 2002: The Tropospheric Biennial Oscillation and Asian-Australian monsoon rainfall. *J. Climate*, **15**, 722-744.
- National Climate Centre, 1999: *98 China severe flood and Climate Anomalies*. Chinese Meteor. Press, 137pp. (in Chinese)
- Shen, Suhung, and K.M. Lau, 1995: Biennial oscillation associated with the East Asian Summer Monsoon and tropical sea surface temperatures. *J. Meteor. Soc. Japan*, **73**, 105-124.
- Torrence, C., and G.P. Compo, 1998: A practical guide to wavelet analysis. *Bull. Amer. Meteor. Soc.*, **79**, 61-78.
- Trenberth, K.E. and Caron, 2000: The Southern Oscillation revisited: Sea Level pressure, surface temperature, and precipitation. *J. Climate*, **13**, 4358-4365.
- Wang, Bin, Renguang Wu, and Xiouhua Fu, 2000: Pacific-east Asian Teleconnection: How does ENSO affect East Asian Climate? *J. Climate*, **13**, 1517-1536.

Table 1. Classification of ENSO years. E0 and E1 denote El Nino onset year and the year immediately following onset respectively. The year immediately following E0 will not be assigned as E1 if the El Nino episode is ended before March. Similar notations are used for La Nina. S, M and W denotes respectively the strength of the episode as strong, moderate and weak.

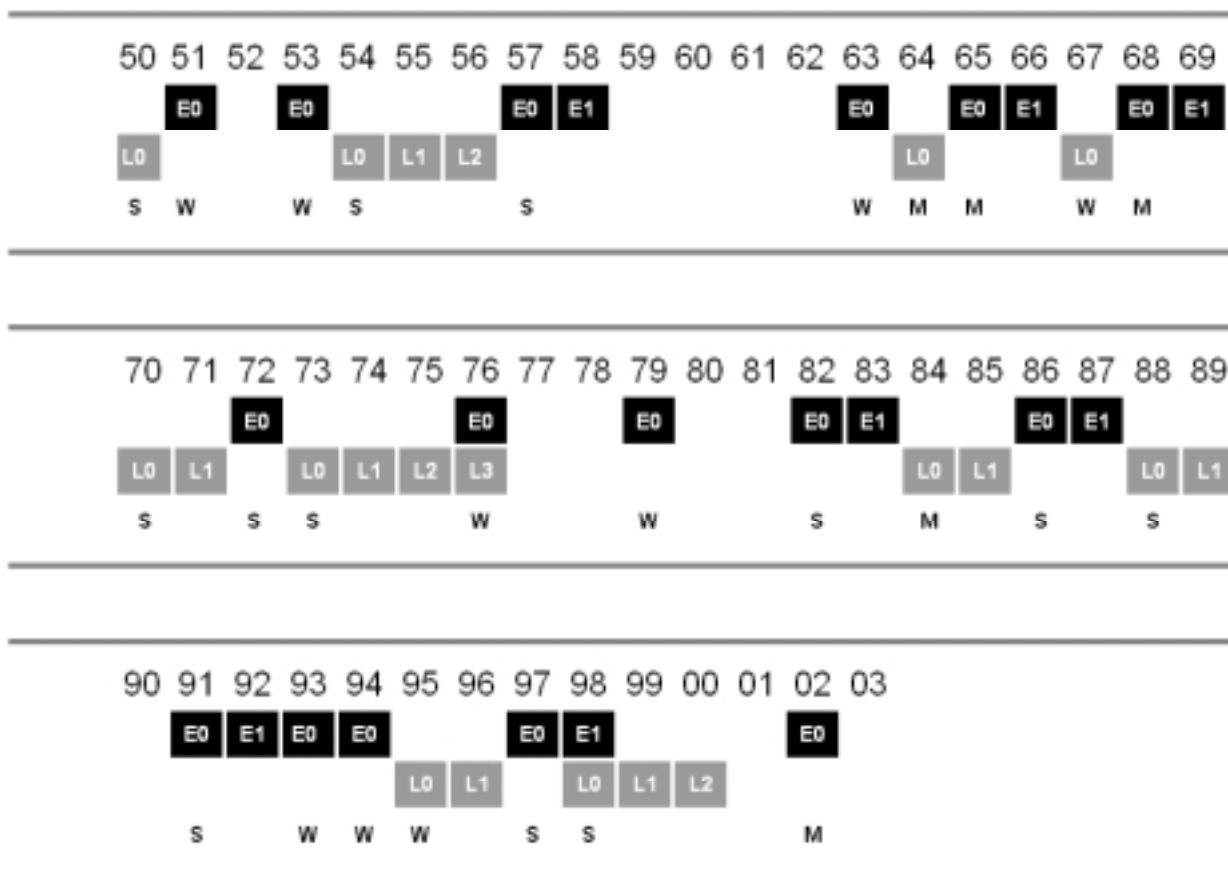


Table 2. Statistics of the annual rainfall in Hong Kong for different ENSO conditions (1950-2003).

ENSO status	Annual rainfall		
	Below normal	Near normal	Above normal
Strong E0	1	1	4
E1	1	3	3
L1	2	5	0

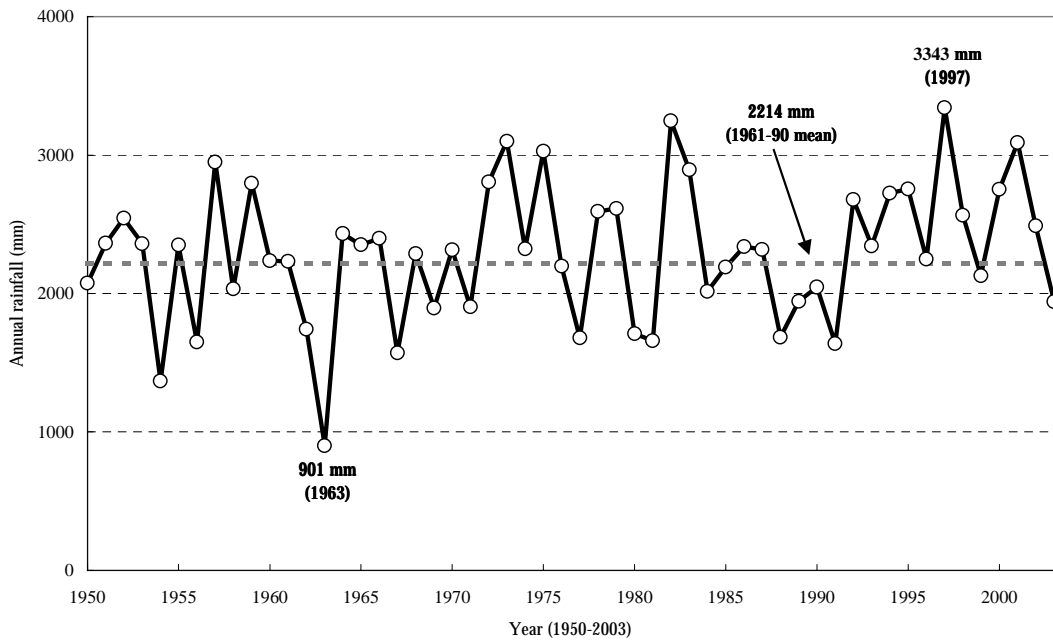


Figure 1. Time series of the annual rainfall in Hong Kong.

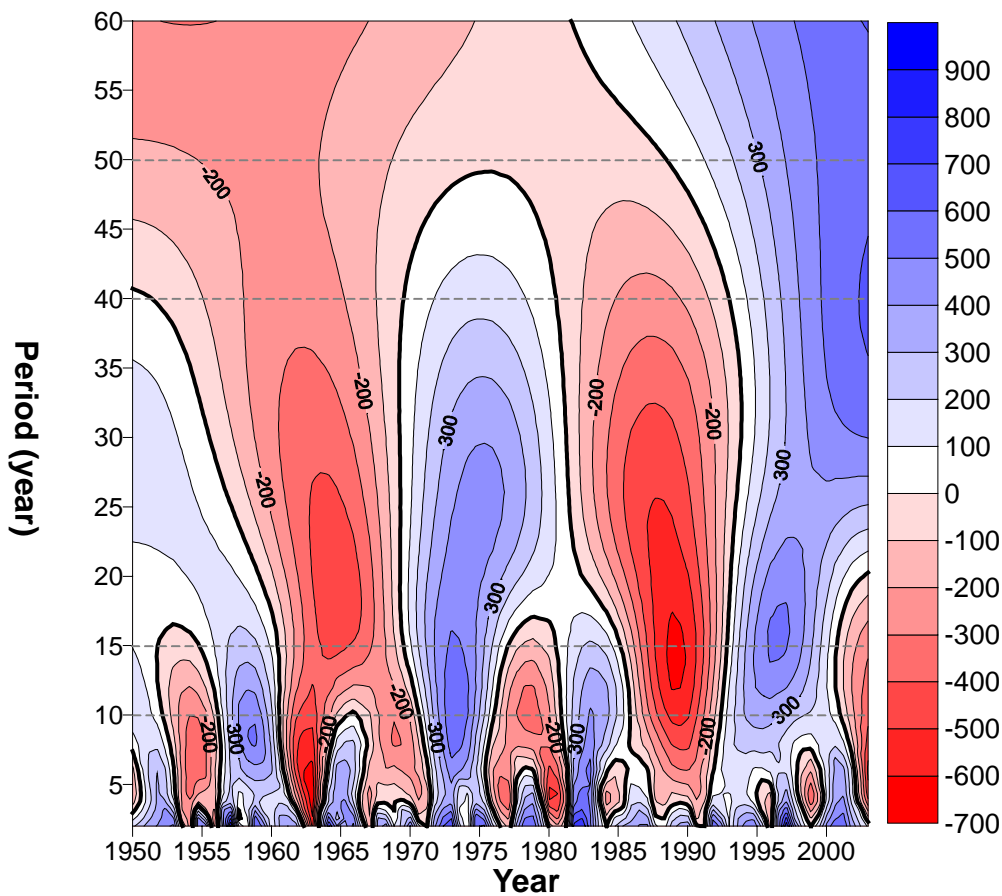


Figure 2. Wavelet analysis of the annual rainfall in Hong Kong. The numbers marked along the isolines are the wavelet transform coefficients. The higher the absolute value, the stronger the signal.

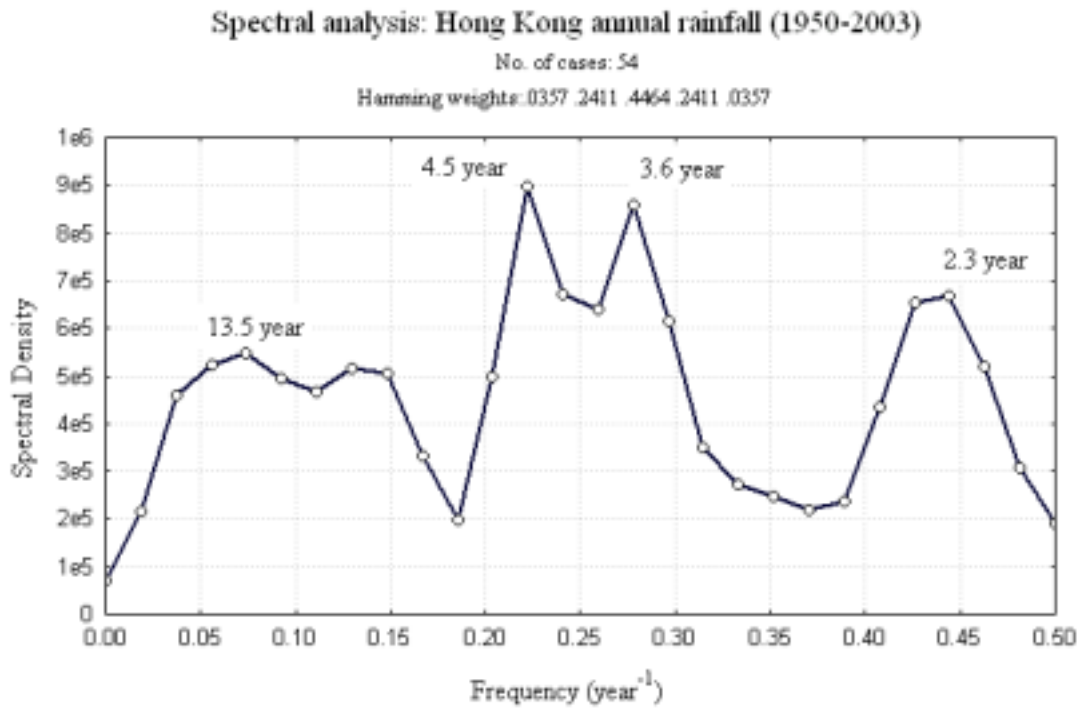


Figure 3. Spectral analysis of the annual rainfall in Hong Kong.

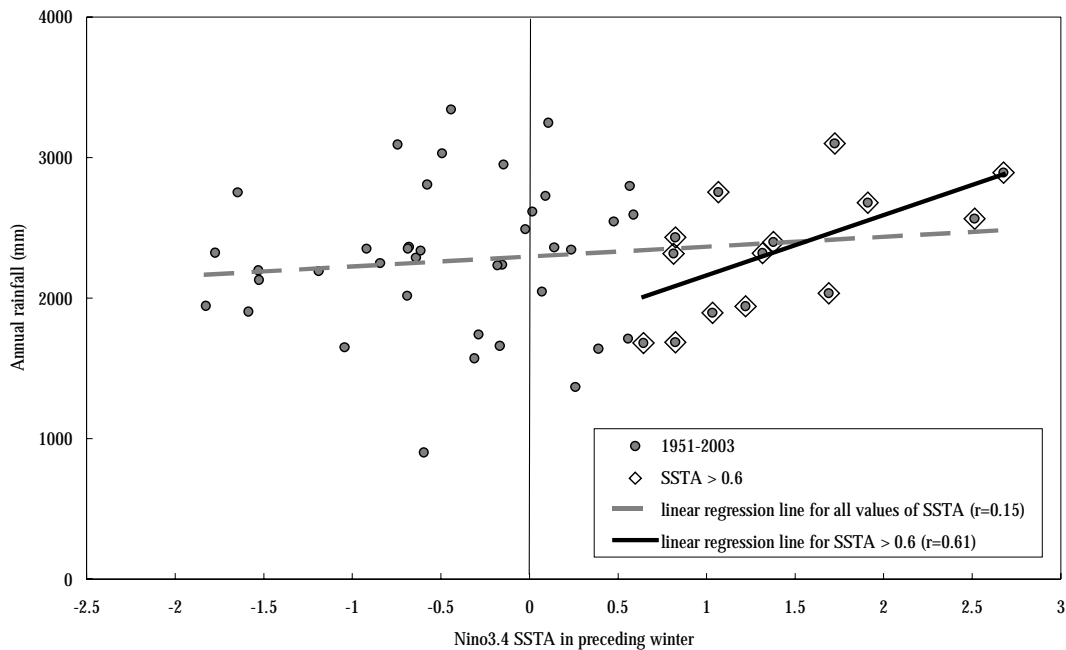


Figure 4. Scatter diagram showing the relationship between the annual rainfall in Hong Kong and the Nino-3.4 sea surface temperature anomaly (SSTA) in the preceding winter. Significant correlation is noted when SSTA > 0.6 °C such that the warmer the SST in the equatorial central Pacific, the more the annual rainfall in Hong Kong.

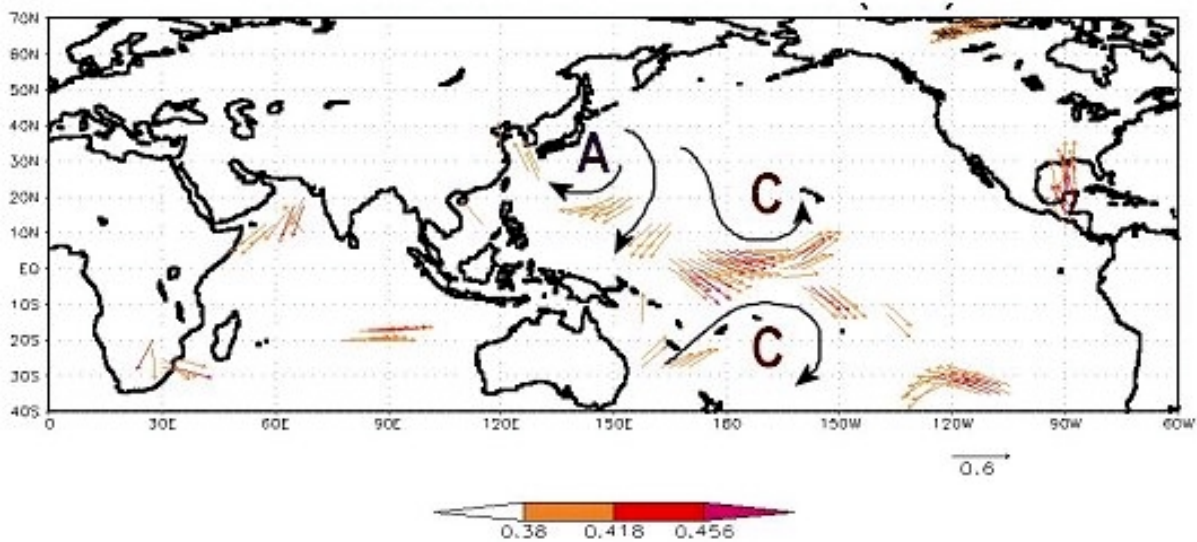


Figure 5. Correlation between the annual rainfall in Hong Kong and the 850 hPa wind in the preceding winter. The u-component and v-component of the vector represents the correlation of the annual rainfall with the 850 hPa zonal and the meridional wind respectively. A and C represent anticyclonic and cyclonic circulations respectively.

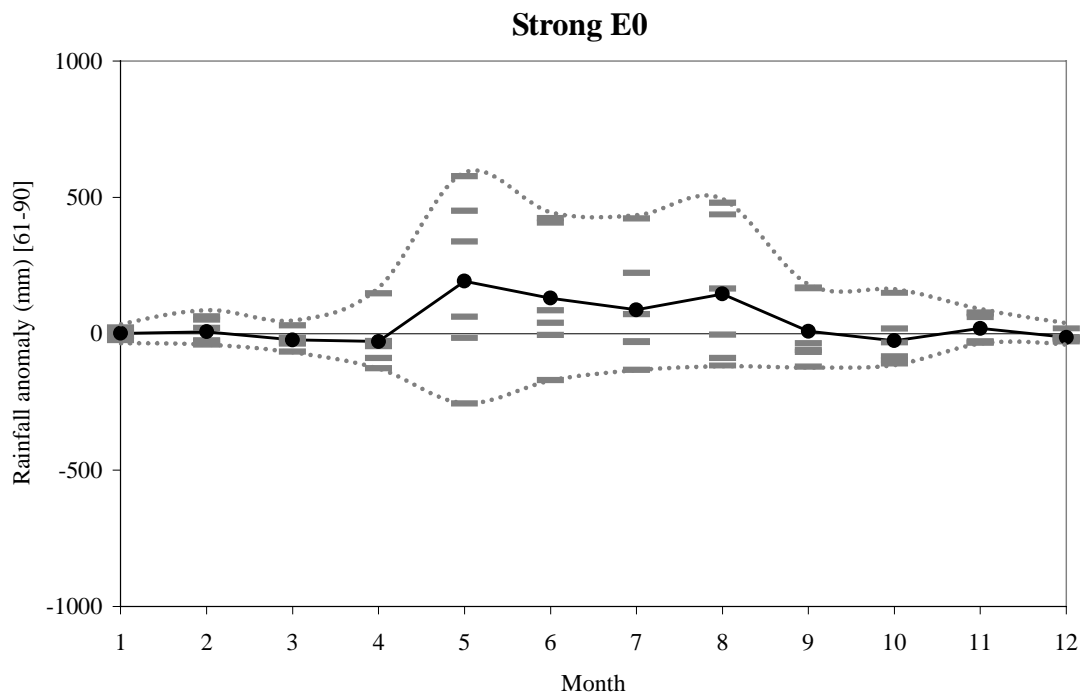


Figure 6. Monthly rainfall anomalies in Hong Kong for strong El Niño onset years (E0). Each horizontal bar represents the monthly rainfall anomaly in a year. The bolded line is the profile of the average monthly rainfall anomaly. The dotted lines are the envelope of the monthly rainfall anomaly.

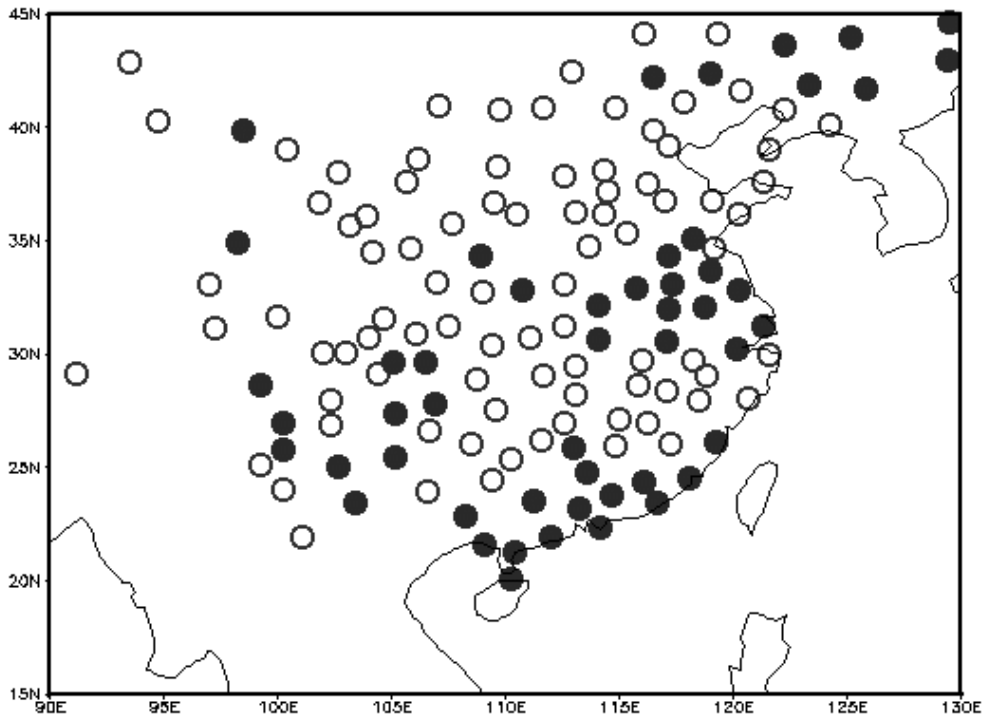


Figure 7 Rainfall anomalies in China during May-August for strong El Niño onset years (E0). For each station, positive (negative) anomaly is indicated by black (open) circle. The rainfall data (1951-2000) are sourced from the National Climate Centre, China Meteorological Administration.

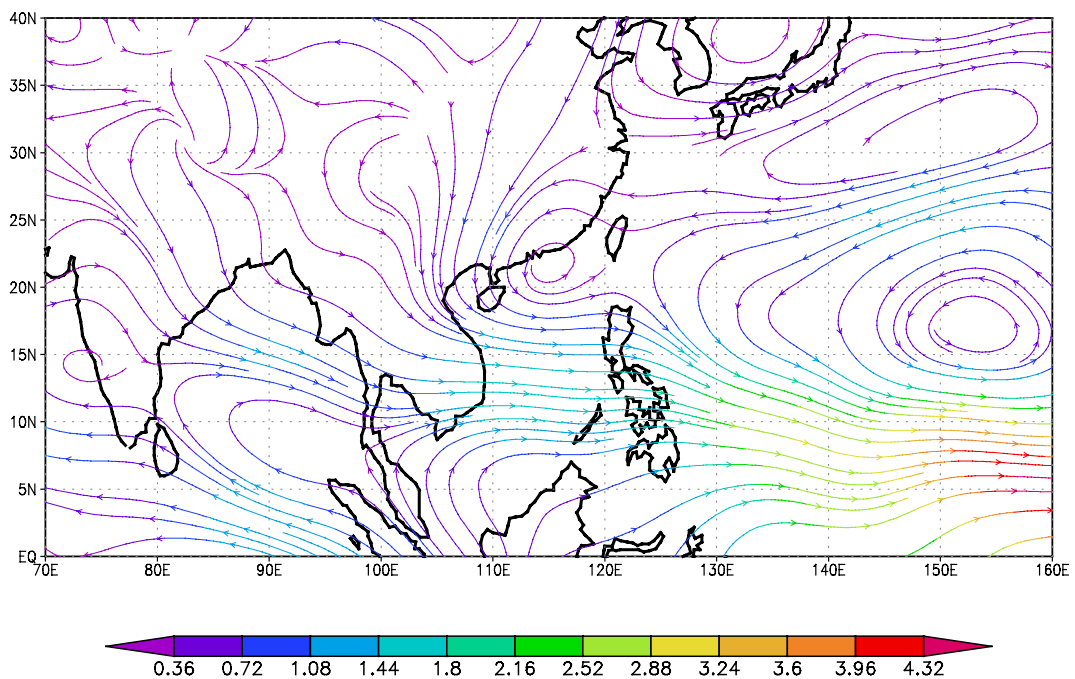


Figure 8. 850 hPa wind anomalies during May-August for strong El Niño onset years (E0). The colour code represents wind speed anomaly in m/s.

# E1

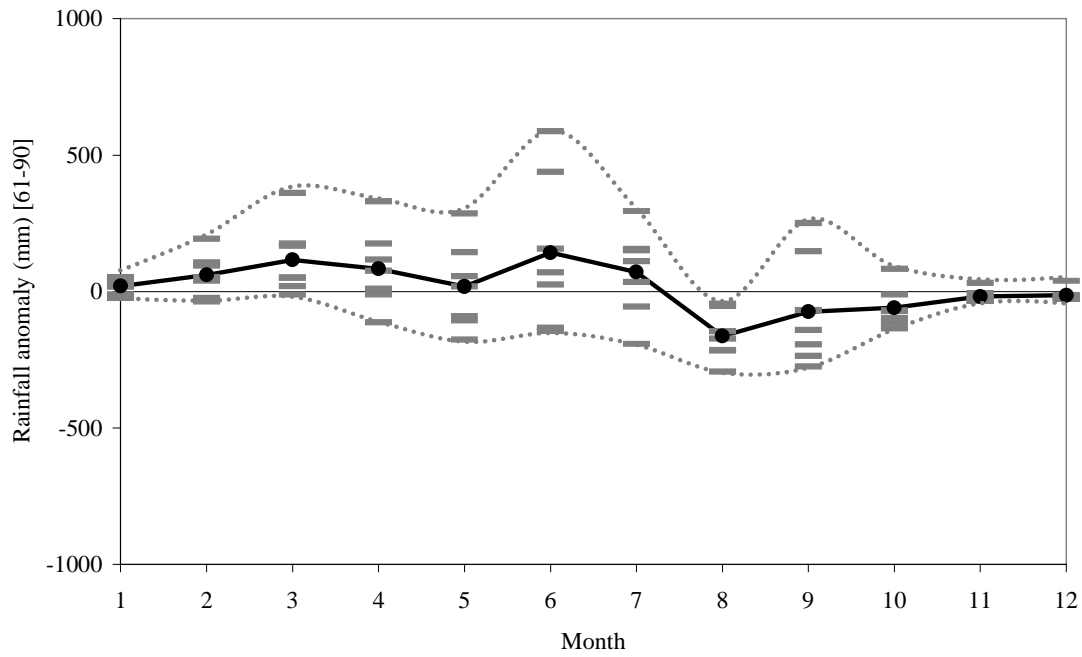


Figure 9. Monthly rainfall anomalies in Hong Kong for the years immediately following El Niño onset (E1). Each horizontal bar represents the monthly rainfall anomaly in a year. The bolded line is the profile of the average monthly rainfall anomaly. The dotted lines are the envelope of the monthly rainfall anomaly.

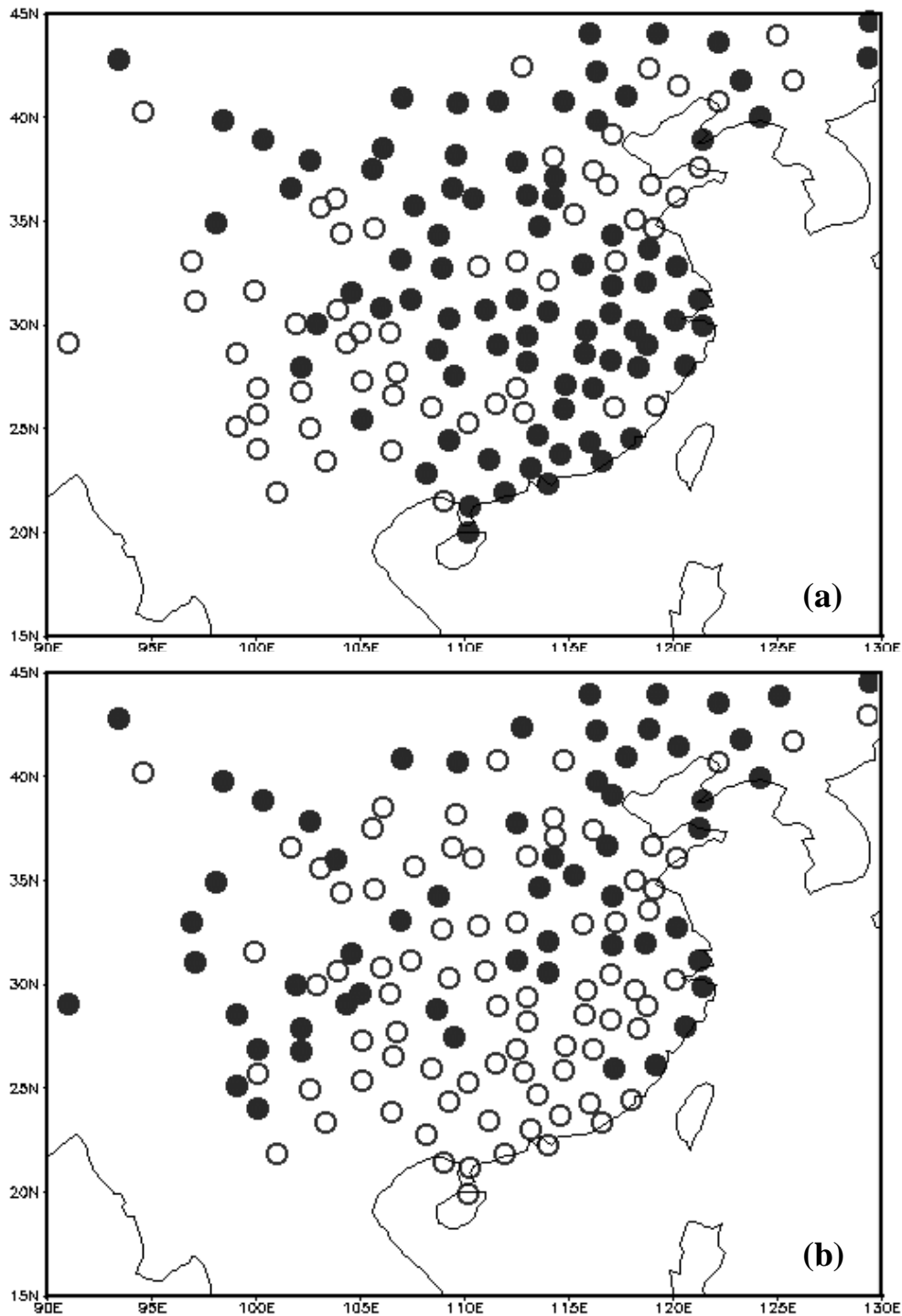


Figure 10. Rainfall anomalies in China during (a) February-July and (b) August-October for the years immediately following El Nino onset (E1). For each station, positive (negative) anomaly is indicated by black (open) circle. The rainfall data (1951-2000) are sourced from the National Climate Centre, China Meteorological Administration.

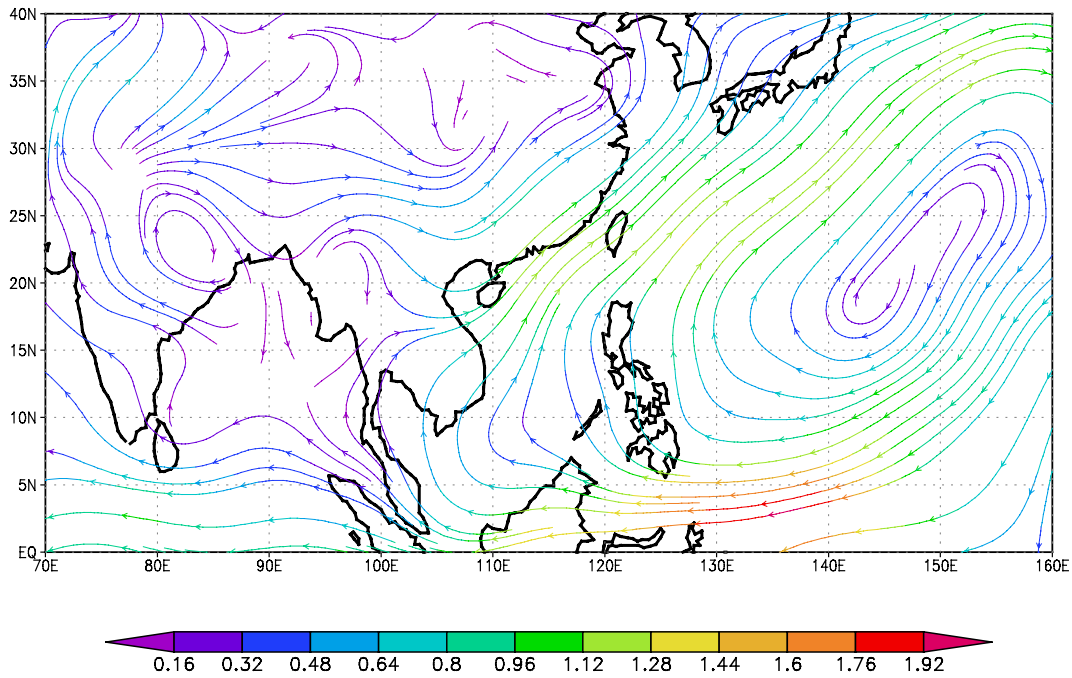


Figure 11. 850 hPa wind anomalies during February-July for the years immediately following El Nino onset (E1). The colour code represents wind speed anomaly in m/s.

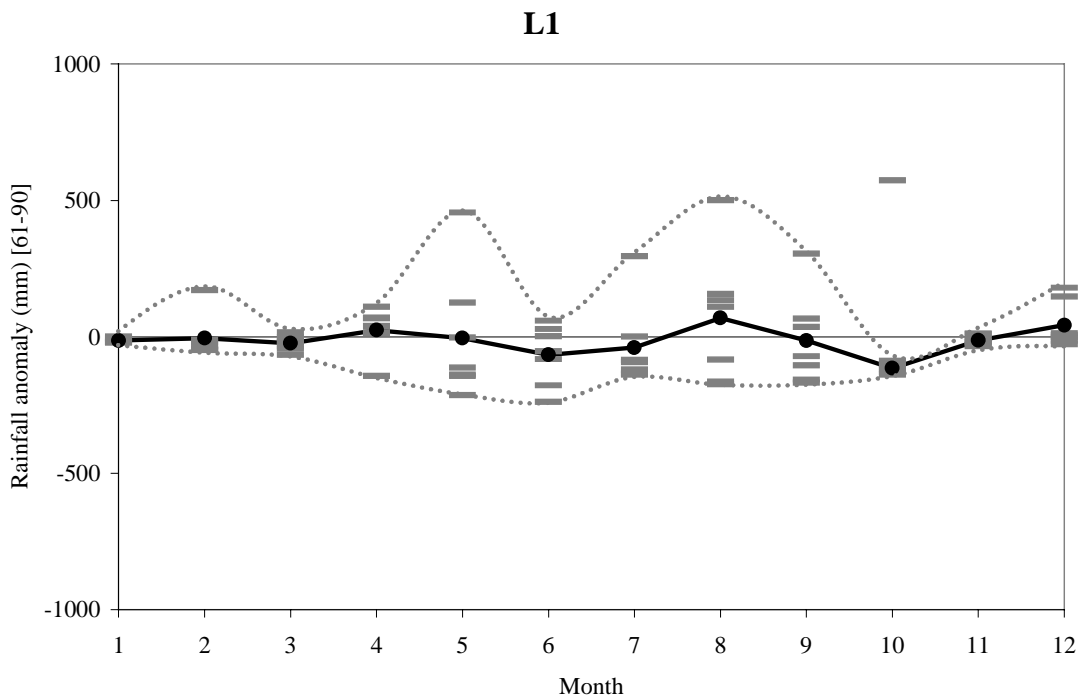


Figure 12. Monthly rainfall anomalies in Hong Kong for the years immediately following La Nina onset (L1). Each horizontal bar represents the monthly rainfall anomaly in a year. The bolded line is the profile of the average monthly rainfall anomaly. The dotted lines are the envelope of the monthly rainfall anomaly.

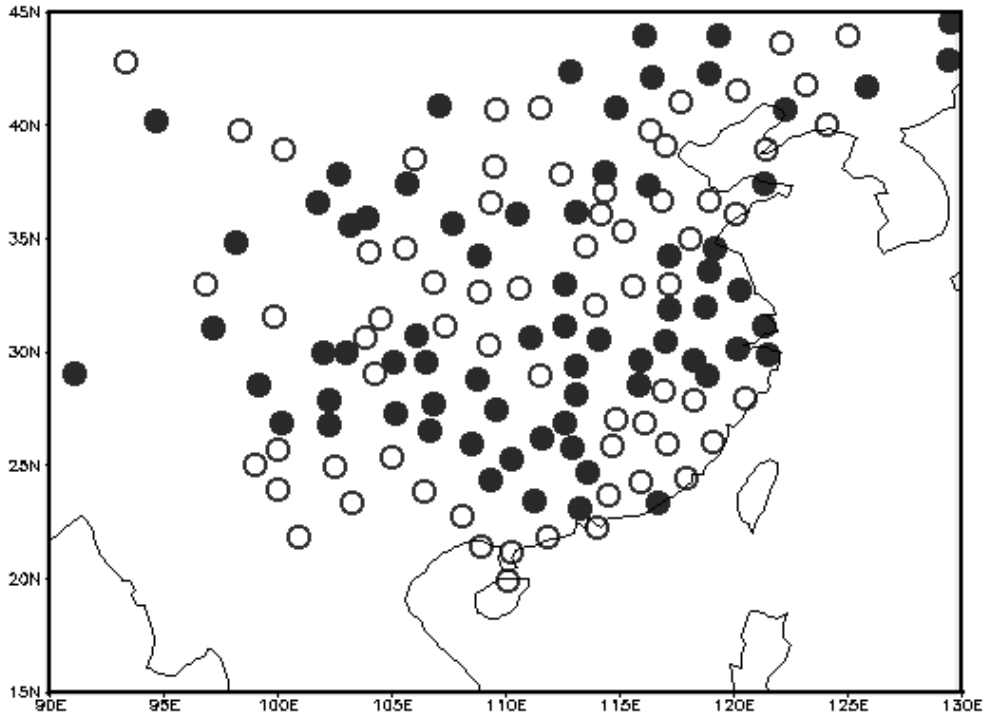


Figure 13. Rainfall anomalies in China during June-July for the years immediately following La Nina onset (L1). For each station, positive (negative) anomaly is indicated by black (open) circle. The rainfall data (1951-2000) are sourced from the National Climate Centre, China Meteorological Administration.

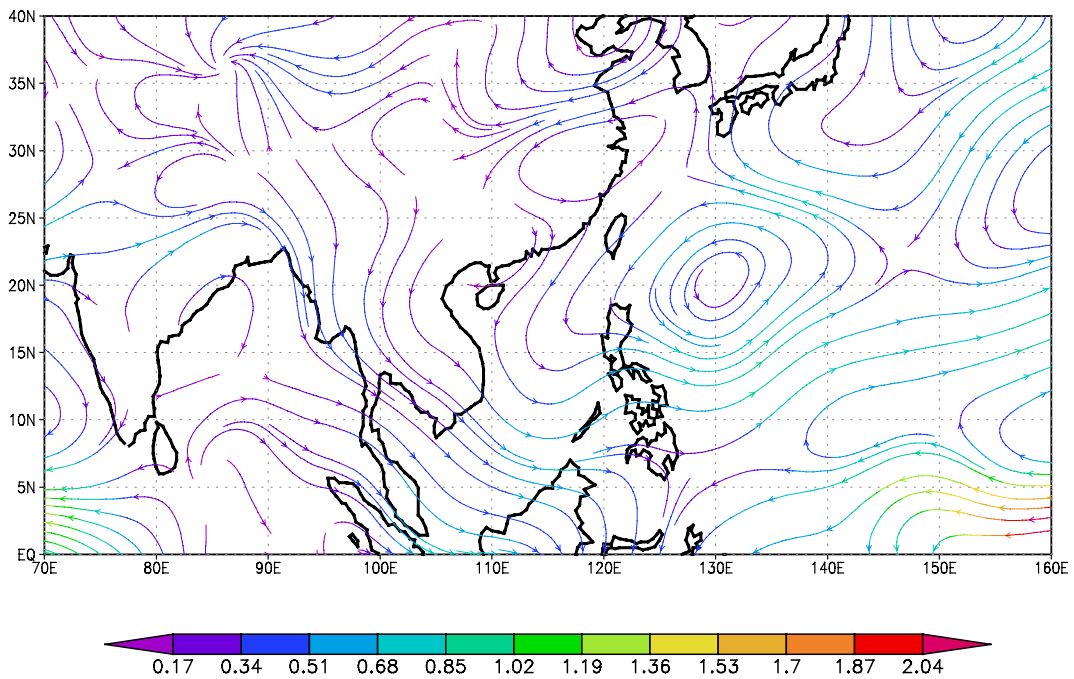


Figure 14. 850 hPa wind anomalies during June-July for the years immediately following La Nina onset (L1). The colour code represents wind speed anomaly in m/s.

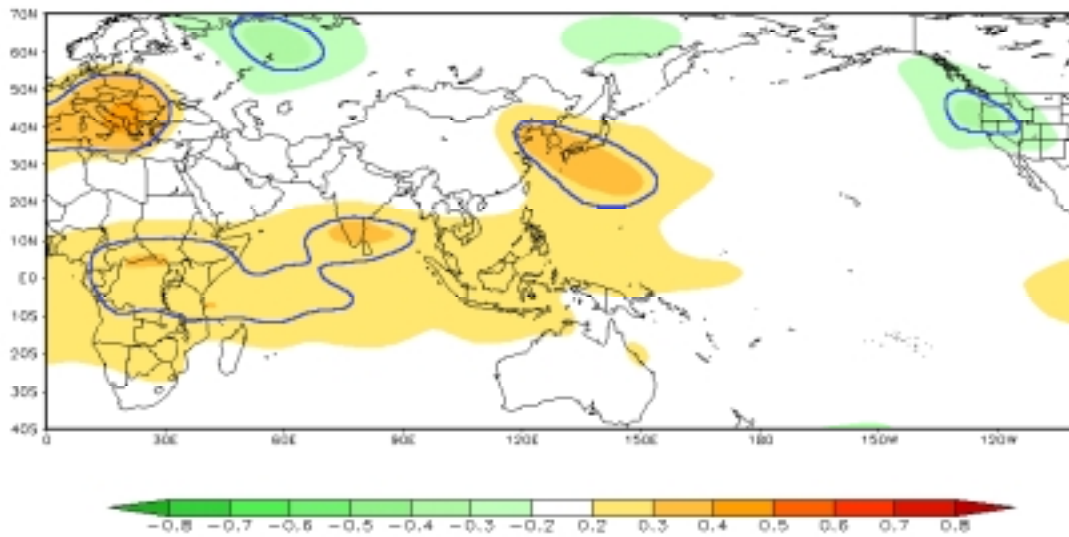


Figure 15. Correlation between the annual rainfall in Hong Kong and 500 hPa geopotential height in the preceding winter. Blue line highlights area with correlation that is statistically significant at 0.05 level.

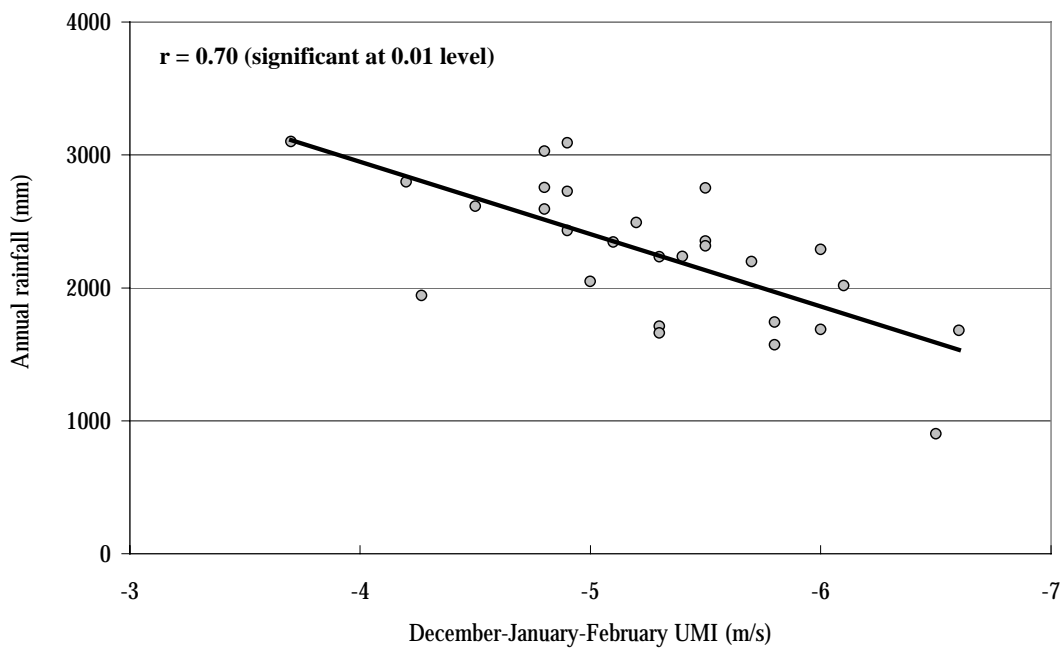


Figure 16. Scatter diagram showing the relationship between the annual rainfall in Hong Kong and winter UMI. The data between 1958 and 2003 are used. Strong E0, E1 and L1 years have been excluded.

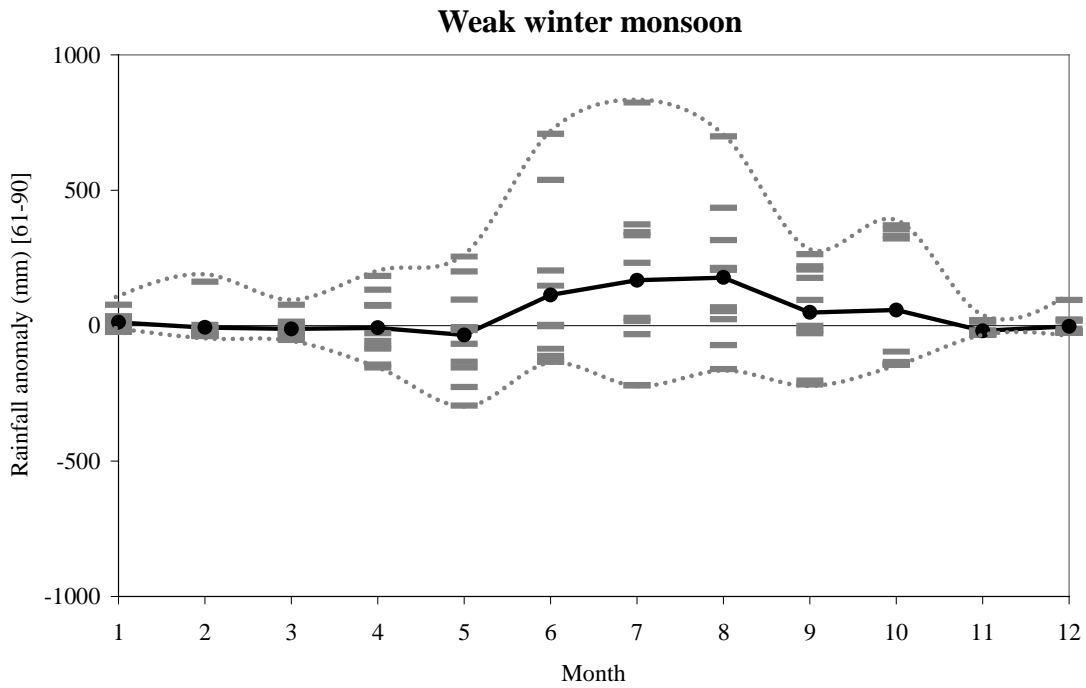


Figure 17. Monthly rainfall anomalies in Hong Kong for the years immediately following weak winter monsoon (excluding strong E0, E1 and L1). Each horizontal bar represents the monthly rainfall anomaly in a year. The bolded line is the profile of the average monthly rainfall anomaly. The dotted lines are the envelope of the monthly rainfall.

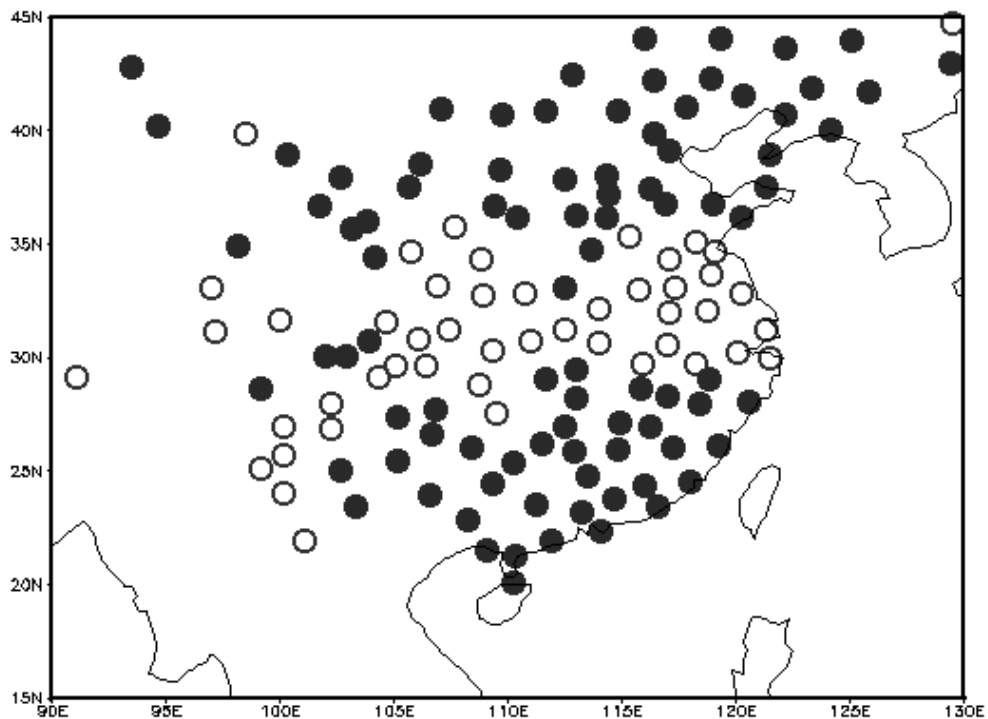


Figure 18. Rainfall conditions in China during June-August for the years immediately following weak winter monsoon. For each station, positive (negative) anomaly is indicated by black (open) circle. The rainfall data (1951-2000) are sourced from the National Climate Centre, China Meteorological Administration.

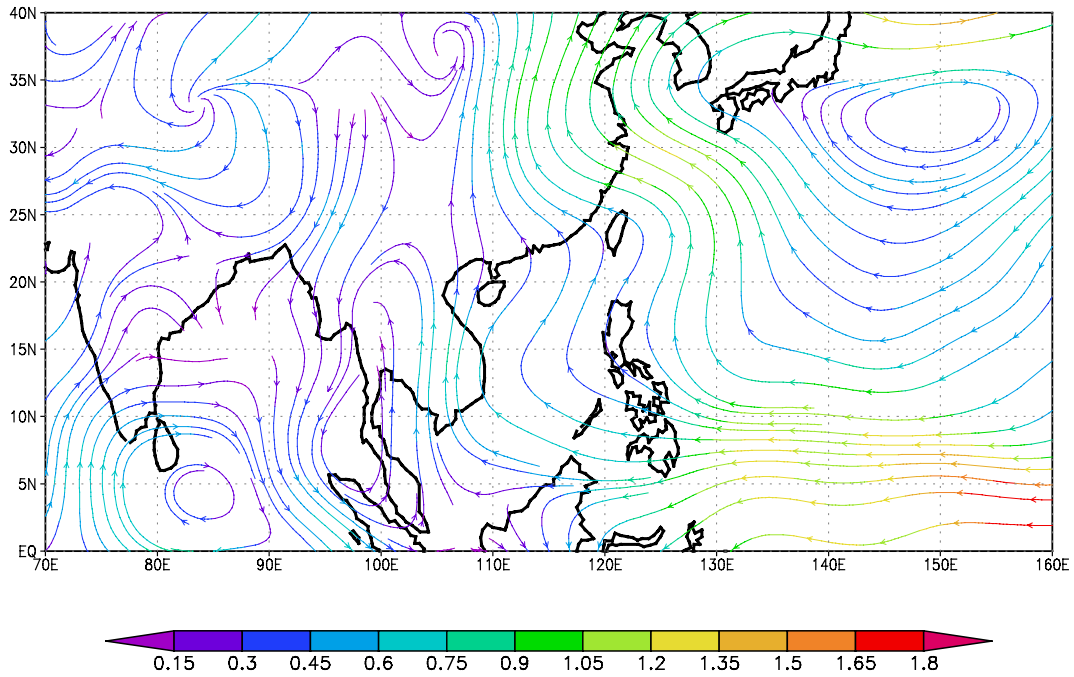


Figure 19. 850 hPa wind anomalies during June-August for the years immediately following weak winter monsoon. The colour code represents wind speed anomaly in m/s.

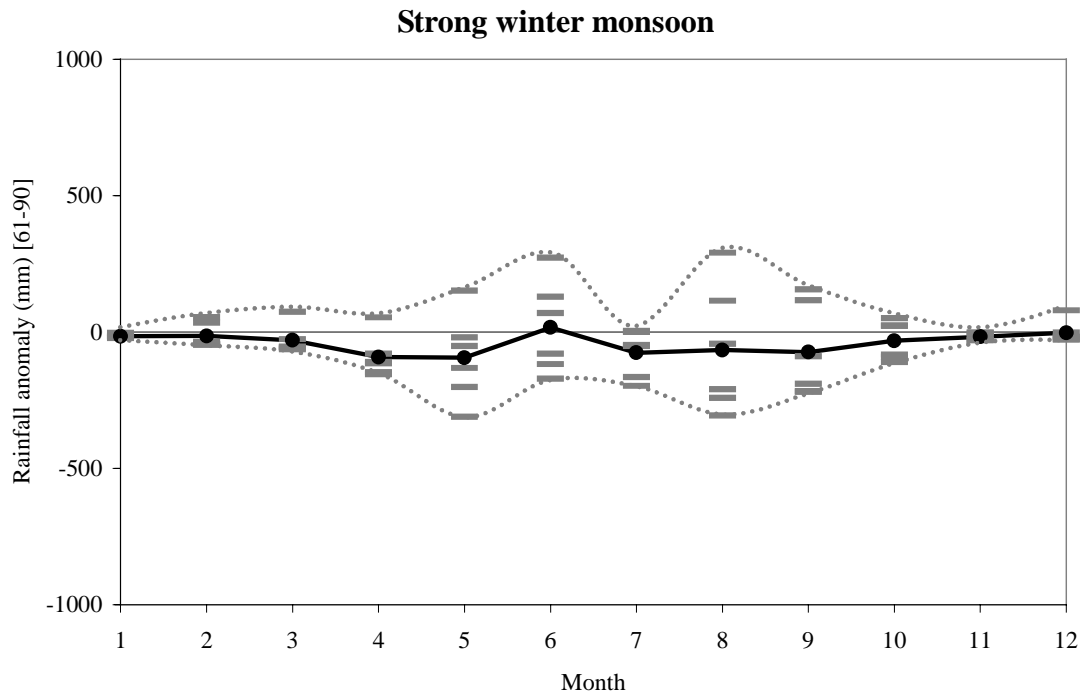


Figure 20. Monthly rainfall anomalies in Hong Kong for the years immediately following strong winter monsoon (excluding strong E0, E1 and L1). Each horizontal bar represents the monthly rainfall anomaly in a year. The bolded line is the profile of the average monthly rainfall anomaly. The dotted lines are the envelope of the monthly rainfall.

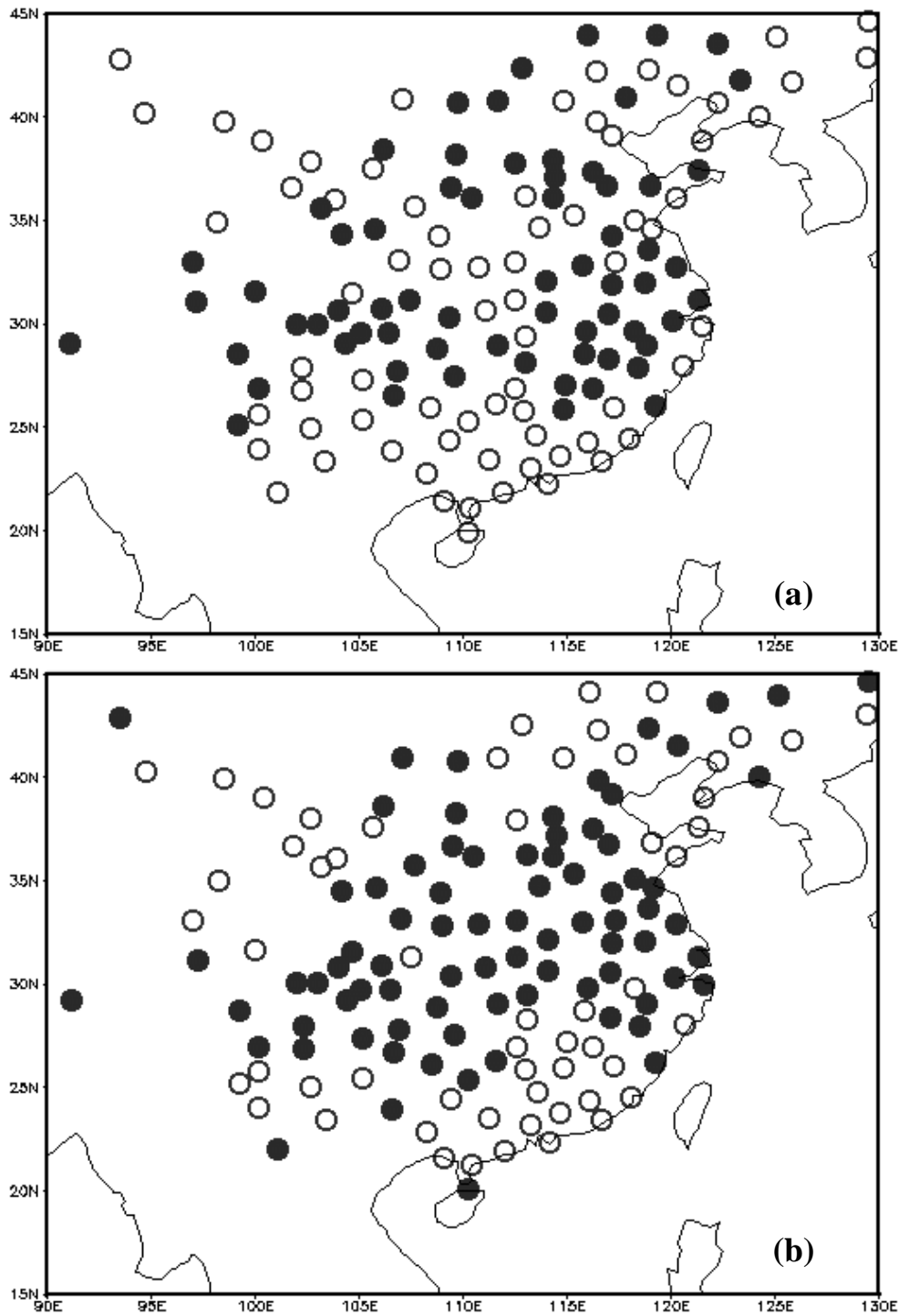


Figure 21. Rainfall anomalies in China during (a) April-May and (b) July-September for the years immediately following strong winter monsoon. For each station, positive (negative) anomaly is indicated by black (open) circle. The rainfall data (1951-2000) are sourced from the National Climate Centre, China Meteorological Administration.

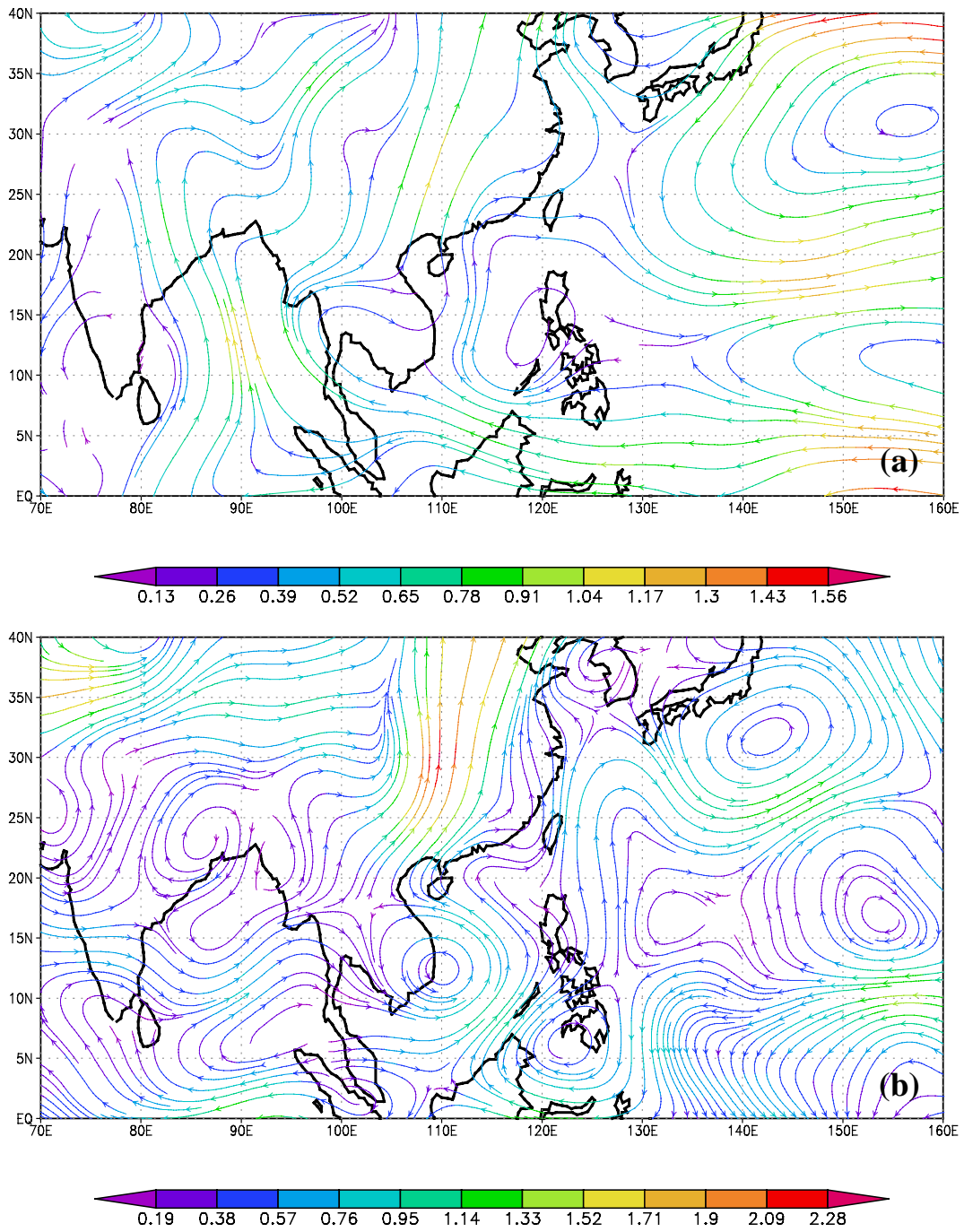


Figure 22. 850 hPa wind anomalies during (a) April-May and (b) July-September for the years immediately following strong winter monsoon. The colour code represents wind speed anomaly in m/s.